Energy and radiative properties of the low-lying NaRb states

A. Zaitsevskii, S. O. Adamson, E. A. Pazyuk, and A. V. Stolyarov
Department of Chemistry, Moscow State University, Moscow 119899, Russia

O. Nikolayeva, O. Docenko, I. Klincare, M. Auzinsh, M. Tamanis, and R. Ferber
Department of Physics, University of Latvia, Riga LV-1586, Latvia

R. Cimiraglia
Dipartimento di Chimica, Universitá di Ferrara, Via Borsari 46, I-44100, Ferrara, Italy
(Received 6 October 2000; published 13 April 2001)

Many-body multipartitioning perturbation theory (MPPT) was applied to calculate the potential energy of 11 lowest electronic states of the NaRb molecule, $A,C\,^1\Sigma^+-X\,^1\Sigma^+$, $B,D\,^1\Pi-X^1\Sigma^+$, $D\,^1\Pi-A\,^1\Sigma^+$ and $D\,^1\Pi-B\,^1\Pi$ transition dipole moments, as well as nonadiabatic L-uncoupling matrix elements between the examined $^1\Pi$ and four lowest $^1\Sigma^+$ states for both $^{23}Na^{85}Rb$ and $^{23}Na^{87}Rb$ isotopomers. The relevant MPPT *ab initio* matrix elements and energy curves were converted by means of the approximate sum rule to radiative lifetimes and Λ-doubling constants (q factors) for the particular rovibronic levels of the $B\,^1\Pi$ and $D\,^1\Pi$ states. The theoretical lifetimes agree well with their experimental counterparts for both $B\,^1\Pi$ and $D\,^1\Pi$ states. The q factor estimates obtained in the singlet-singlet approximation are in good agreement with the experimental ones for the $D\,^1\Pi(1\leqslant v'\leqslant 12; 7\leqslant J'\leqslant 50)$ levels, exhibiting a pronounced difference for the $B\,^1\Pi$ state. Considerably better agreement was achieved by accounting for the spin-orbit perturbation effect caused by the near-lying $c^3\Sigma^+$ state. Relative intensity distributions in the $D\,^1\Pi\rightarrow X\,^1\Sigma^+$ dispersed fluorescence spectra excited by fixed Ar^+ laser lines were measured for $v'(J')=0(44)$, 1(104), 4(25), 6(44,120), 10(36), and 12(50) $D\,^1\Pi$ levels. The experimental intensities and term values were simultaneously embedded in the nonlinear least-square fitting procedure to refine the $D\,^1\Pi$ potential.

DOI: 10.1103/PhysRevA.63.052504 PACS number(s): 31.10.+z, 33.15.−e, 33.50.Dq, 33.70.Fd

I. INTRODUCTION

The heteronuclear alkali dimers are a permanent challenge to both experimental and theoretical researchers involved in collision dynamics, photoassociative spectra, laser-cooled and trapped alkaline atoms due to their promising prospects for the formation of ultracold molecules [1]. As far as the NaRb molecule is concerned, in spite of a number of experimental and theoretical studies carried out in the last two decades [2–9], the knowledge of its energy and radiative properties is still rather scarce. High accuracy experimental molecular constants and corresponding RKR potentials are available only for the ground $X\,^1\Sigma^+$ state and, to a certain extent, for the bound part of the $a\,^3\Sigma^+$ state correlating to the Na(3s) + Rb(5s) atoms, as well as for the $B\,^1\Pi$ state correlating to the Na(3s) + Rb(5p) atoms due to systematic studies performed in the Katô group [2–5] by polarization spectroscopy and optical-optical double resonance methods. Molecular constants for the $D\,^1\Pi$ state, which are responsible for the strong green $D\,^1\Pi-X\,^1\Sigma^+$ absorption band observed as early as 1928 by Walter and Barrat [10] , were only roughly estimated in [6] from the intensity distribution in the $D\,^1\Pi-X\,^1\Sigma^+$ laser-induced fluorescence (LIF). Potential energies for the ground and 27 lowest excited electronic states of NaRb have been recently calculated [7] by means of non-empirical pseudopotentials, parametrized l-dependent polarization potentials, and the full valence configuration-interaction (CI) method. It should be noted that the agreement between theoretical and available experimental spectroscopic constants is not always good enough, cf. for instance, the calculated value [7] $\omega_e=51.6$ cm^{-1} for the $B\,^1\Pi$ state of $^{23}Na^{85}Rb$ with the experimental one 61.171 cm^{-1} obtained in [2]. The existing information on radiative properties of NaRb is even poorer. Only two fragmentary measurements of the collisionless radiative lifetime are reported in the literature, namely $\tau=17.8$ ns for $B\,^1\Pi$ ($v'=5$, $J'\approx 20$) [5] and $\tau=22.4$ ns for $D\,^1\Pi$ ($v'=0, J'=44$) [8]. An R-independent estimate $\mu=7.0$ D of the $B\,^1\Pi-X\,^1\Sigma^+$ transition dipole moment averaged within the internuclear distance region 3.73 Å$<R<$4.98 Å was obtained in Ref. [5] from the experimental lifetime and LIF intensity distribution. Only a very rough estimate of the relative $\mu(R)$ dependence was suggested in [6] for the $D\,^1\Pi-X\,^1\Sigma^+$ transition. No theoretical calculations of radiative properties of NaRb can be found in literature.

In our recent study on NaRb [9] the permanent electric dipole moments d were measured for a number of v',J' levels of the $B\,^1\Pi$ and $D\,^1\Pi$ states by combining the dc Stark-effect-induced $e-f$ mixing for a particular rovibronic level with the direct determination of its Λ-splitting energy $\Delta_{e,f}$ by means of the electric radio-frequency–optical double resonance (RF-ODR) method. The measured d values were in good agreement with the concomitant *ab initio* calculations performed in [9] by the multipartitioning perturbation theory (MPPT) developed in [11,12]. The MPPT method has been previously approved as an excellent tool to calculate permanent electric dipoles [13] and transition dipole moments [14] in the NaK molecule. What is more, in Ref. [15] the MPPT was adapted to calculate the electronic

L-uncoupling matrix elements $L_{\Pi\Sigma}(R)$ between the sampled $^1\Pi$ and remote $^1\Sigma$ states, providing reliable estimates of the Λ-splitting energy and the q factors of the $B\,^1\Pi$ and $D\,^1\Pi$ states of NaK.

The main goals of the present work are as follows. First, to apply the MPPT techniques developed and approved in [9,11,12,15] to evaluate NaRb potential-energy curves $U(R)$ of the electronic states converging to the first three dissociation limits, as well as of the $E\,^1\Sigma^+$ state. Second, to calculate the transition dipole moments $\mu(R)$ for the singlet-singlet transitions, as well as the nonadiabatic L-uncoupling matrix elements $L_{\Pi\Sigma}(R)$ between the examined $^1\Pi$ state and four lowest $^1\Sigma^+$ states for both $^{23}Na^{85}Rb$ and $^{23}Na^{87}Rb$ isotopomers. To allow direct comparison with available experimental results, the relevant MPPT matrix elements and potential-energy curves were converted to the radiative lifetimes and Λ-doubling constants (q factors) for the particular rovibronic levels of the $B\,^1\Pi$ and $D\,^1\Pi$ states by using the approximate sum rule [16]. In addition, the relative intensity distributions in the $D\,^1\Pi \rightarrow X\,^1\Sigma^+$ dispersed fluorescence spectra were measured and embedded, together with the transition dipole moment function $\mu_{D\,^1\Pi - X\,^1\Sigma^+}(R)$ computed by the MPPT, the high-accurate RKR $X\,^1\Sigma^+$ potential [5], and experimental $D\,^1\Pi(v',J')$ rovibronic term values, in a nonlinear least-square fitting procedure to refine the $D\,^1\Pi$ potential.

II. METHOD

A. Experiment

In this paper we present three experimental data sets on the NaRb molecule obtained from the laser-induced fluorescence measurements, namely, the $D\,^1\Pi$ state term values for a number of rovibronic v',J' levels, and relative intensity distributions in the $D\,^1\Pi \rightarrow X\,^1\Sigma^+$ LIF progressions originating from these levels, as well as Λ-doubling constants for v',J' levels of the $B\,^1\Pi$ and $D\,^1\Pi$ states. The experimental setup has been described in more detail in our previous papers [13,14]. Let us review here some essential points. The fixed frequency lines of the Spectra Physics 171 Ar^+ laser, as well as of Kr^+ and He-Ne lasers were used to excite a particular v',J' level of the $D\,^1\Pi$ or $B\,^1\Pi$ state of the NaRb molecules in a thermal cell made from the alkali-metal-resistant glass. The cell was connected to the vacuum pump and contained the mixture of Na:Rb metals in the respective mass ratio ca. 1:4 at temperature $T \approx 550$ K.

Term values. The $D\,^1\Pi$ state rovibronic term values $T^{exp}_{v'J'}$ were obtained by adding the $D\,^1\Pi(v',J') \leftarrow X\,^1\Sigma^+(v'',J'')$ transition laser frequency to the energy of the absorbing ground-state rovibronic level v'',J''. The assignment of the v, J quantum numbers belonging to the particular isotopomer $^{23}Na^{85}Rb$ or $^{23}Na^{87}Rb$ is discussed in more detail in Ref. [9]. It is based on the careful measurements of the vibrational and rotational spacings in LIF progressions and their comparison with the spacings calculated using the high-accurate ground-state molecular constants given in Refs. [2,5]. Vibrational numbering was supported by a comparison of the LIF relative intensity distribution with the calculated Franck-Condon factors. In addition to the $D\,^1\Pi$ state $v'(J')$ levels listed in Table I of Ref. [9], we have identified two more $v'(J')$ levels, namely $1(J' \approx 104)$ and $6(J' \approx 120)$, excited by the 514.5-nm Ar^+-laser line. However, we do not present here the term values of these states since, because of poor accuracy of ground-state term values for large J', the latter was only estimated, and, consequently it was impossible to assign the particular isotopomer. Nevertheless, the respective LIF progressions were involved in the relative intensity distribution analysis.

Intensity distributions. The $D\,^1\Pi \rightarrow X\,^1\Sigma^+$ relative intensity distributions were measured in the photon-counting regime by detecting LIF spectra from the $D\,^1\Pi(v',J')$ levels excited by single-mode Ar^+-laser lines. The double monochromator with the slits 0.08–0.10 mm provided 0.3–0.4 Å spectral resolution. In order to avoid the temperature drift and laser excitation condition changing effects, the measurements were performed in a step-by-step regime by alternative returning to the particular fluorescence line of the same progression that served as a reference line. The spectral sensitivity of the registration system was calibrated using a standard tungsten bandlamp with the known spectral irradiance at definite temperature. To avoid the possible influence of the linear polarization of the molecular fluorescence, the polarization vector of the exciting laser beam was directed along the observation direction.

Λ-splitting constants. The experimental Λ-splitting energy values $\Delta_{e,f}$, measured directly by the RF-ODR method [17,18], are presented in Table I of Ref. [9]. These values have been used in the present work to extract the Λ-splitting constants, or q factors. Note that this method yields only the absolute value and not the sign of the q factor.

B. Outline of theory

The present theoretical study of the NaRb molecule is based on the *ab initio* electronic structure calculations performed by means of the many-body multipartitioning perturbation theory (MPPT) [11,12]. The transition moments $\mu(R)$, as well as the L-uncoupling matrix elements $L_{\Pi\Sigma}(R) = \langle \Pi | L^{\pm} | \Sigma^{\pm} \rangle$ between the $^1\Pi$ state under study and the remote $^1\Sigma^{\pm}$ states were determined via the perturbative spin-free one-electron transition density matrices. The scalar (spin-independent) relativistic effects have been taken into account by replacing the inner-core shells with the averaged relativistic pseudopotentials [21,22], leaving nine electrons of each atom for explicit treatment. The performed calculations employ the MPPT to incorporate effective interactions arising from the core-valence correlations and core-polarization effects into the model-space CI (valence-shell full CI) problem. The completeness of the model space guarantees the size consistency of the derived energies and matrix elements. The spin-orbit (SO) interaction effects on the electronic properties under study were neglected in the present treatment. The computational details can be found elsewhere [9,15]. The transition moment functions were obtained in the dipole-length approximation; the mass-dependent L-uncoupling matrix elements were computed separately for the $^{23}Na^{85}Rb$ and $^{23}Na^{87}Rb$ isotopomers. The

required atomic masses of the Na and Rb isotopes were taken from Ref. [19]. For Π-Σ transitions $\mu_{\Pi\Sigma}(R)$ and $L_{\Pi\Sigma}(R)$ functions relate to each other as [20]

$$L_{\Pi\Sigma}^{^{23}\mathrm{Na}^{87}\mathrm{Rb}} - L_{\Pi\Sigma}^{^{23}\mathrm{Na}^{85}\mathrm{Rb}} = \xi\mu_{\Pi\Sigma}[U_\Pi - U_\Sigma], \tag{1}$$

where $\xi=\xi(R)$ is the shift of the center of mass and $U_\Pi(R)-U_\Sigma(R)\equiv\Delta U_{\Pi\Sigma}(R)$ is the difference of the Born-Oppenheimer potentials. Due to the small shift of the center of mass for two isotopomers, the calculated differences of the isotopic-substituted L-uncoupling matrix elements are obviously expected to be very small. Nevertheless, to test self-consistency of the calculated *ab initio* U, μ, and L values, the relation (1) was applied to evaluate the corresponding $\mu_{\Pi\Sigma}$ moments and to compare them with their dipole-length analogs.

The splitting Δ_{ef} between e and f components of the initially degenerated $^1\Pi$ level is mainly determined by *regular* electronic-rotational perturbations caused by the remote singlet $^1\Sigma^\pm$ states [23]. Under this *singlet-singlet approximation*, strong J dependence of the Δ_{ef} values is usually reduced to the so-called q factors using the expression $\Delta_{ef}^\Pi = q_{vJ}^\Pi J(J+1)$ [20]. The expression for the q factor is

$$q_{vJ}^\Pi = \frac{1}{2M^2}\sum_\Sigma (-1)^k \sum_{v_\Sigma} \frac{|\langle v_J^\Pi | L_{\Pi\Sigma}/R^2 | v_J^\Sigma\rangle|^2}{T_{vJ}^\Pi - T_{v'J}^\Sigma}, \tag{2}$$

where M is the reduced molecular mass, and $k=0$ and 1 for the Σ^+ and Σ^- states, respectively. The rovibronic term values T_{vJ} and wave functions $|v_J\rangle$ are the eigenvalues and eigenfunctions of the respective radial Schrödinger equation.

The radiative lifetimes $\tau_{iv'J'}$ and relative $iv'J'\rightarrow jv''J'$ fluorescence intensities $I_{ij}^{v'J'v''J''}$ combine with each other through the Einstein coefficients $A_{ij}^{v'J'v''J''}$ [23]

$$\tau_{iv'J'}^{-1} = \sum_{jv''J''} A_{ij}^{v'J'v''J''}, \quad I_{ij}^{v'J'v''J''} = A_{ij}^{v'J'v''J''}/A_{ij}^{v'J'v''_{max}J''}, \tag{3}$$

$$A_{ij}^{v'J'v''J''} = \frac{8\pi^2}{3\hbar\epsilon_0}(T_{iv'J'} - T_{jv''J''})^3 |\langle v'_{J'}|\mu_{ij}(R)|v''_{J''}\rangle|^2 \times \frac{S_{J'J''}}{2J'+1}, \tag{4}$$

where $S_{J'J''}$ is the Hönl-London factor, v''_{max} corresponds to the band with the maximum intensity within a given progression, $8\pi^2/3\hbar\epsilon_0 = 2.026\times10^{-6}$, ϵ_0 is the permittivity of vacuum, μ_{ij} is in a.u., and T_{ij} are the rovibronic term values in cm^{-1}.

The relevant MPPT transition dipole moments were converted into radiative lifetimes τ_{vJ}^Π for the particular rovibronic levels of the $B\,^1\Pi$ and $D\,^1\Pi$ states by applying the approximate sum rule [16,24], which allows one to avoid tedious summation over vibrational levels of the remote electronic states

$$1/\tau_{vJ}^\Pi \approx \langle v_J^\Pi | A^{sum} | v_J^\Pi\rangle, \quad A^{sum} = \frac{8\pi^2}{3\hbar\epsilon_0}\sum_j \Delta U_{\Pi j}^3 \mu_{\Pi j}^2, \tag{5}$$

$\Delta U_{\Pi j} = U_\Pi - U_j$ being the potential difference between interacting states. Similarly, the L-uncoupling electronic matrix elements $L_{\Pi\Sigma}$ were converted into q factors through

$$q_{vJ}^\Pi \approx \langle v_J^\Pi | Q^{sum} | v_J^\Pi\rangle, \quad Q^{sum} = \sum_{j=\Sigma} Q_j = \frac{1}{2M^2}\sum_{j=\Sigma}(-1)^k \frac{L_{\Pi j}^2}{R^4 \Delta U_{\Pi j}}. \tag{6}$$

The reliability of the sum rules was confirmed numerically by performing the direct summation in Eqs. (2) and (3) for the $D\,^1\Pi$–$B\,^1\Pi$ and $B\,^1\Pi$–$C\,^1\Sigma^+$ pairs possessing minimum energy gap at the internuclear distances of interest. The discrepancy between the results obtained directly and their sum rule analogs is found to be less than 0.1% for all rovibronic levels under consideration. The rovibrational wave functions were calculated using the empirical RKR potentials corresponding to the molecular constants from Ref. [2] for the $B\,^1\Pi$ state and the ones obtained in the present work for the $D\,^1\Pi$ state. The energy differences $\Delta U_{^1\Pi - X\,^1\Sigma^+}$ were evaluated using the corresponding RKR potentials and experimental electronic energies (T_e), while the differences $\Delta U_{^1\Pi - A,C,E\,^1\Sigma^+}$ have been calculated using the present *ab initio* potentials since the experimental molecular constants for the excited $^1\Sigma^+$ states have not been obtained yet. The infinite summation in expression (6) over all possible $^1\Sigma^\pm$ electronic states, including those embedded into the autoionization continuum, was truncated on the $E\,^1\Sigma^+$ state since the large potential differences and the factor R^{-4} in the right-hand side of Eq. (6) suppress significantly the contributions from the remaining remote states [15].

Relative intensity distributions in the LIF progressions are determined by the potential curves of the combining states, as well as by the R dependence of the corresponding transition moment. Therefore, a knowledge of the *ab initio* $\mu_{ij}(R)$ function and experimental molecular constants for the ground state, along with relevant transition frequency measurements, provides the possibility of applying relative intensity measurements to refine a potential curve for the upper state. Since the number of the $D\,^1\Pi$ state term values experimentally obtained in the present work is definitely insufficient to determine a set of $D\,^1\Pi$ molecular constants of reasonable accuracy, both experimental term values $T_{D\,^1\Pi}^{exp}$ and LIF intensity distributions I_{D-X}^{exp} were simultaneously embedded in the weighted nonlinear least-square fitting procedure,

$$\min \sum_{v'J'}\left[\left(\frac{T_{D\,^1\Pi}^{exp} - T_{D\,^1\Pi}^{cal}}{\delta T_{D\,^1\Pi}^{exp}}\right)^2 + \sum_{v''J''}\left(\frac{I_{D-X}^{exp} - I_{D-X}^{cal}}{\delta I_{D-X}^{exp}}\right)^2\right], \tag{7}$$

where the variation parameters are the $D\,^1\Pi$ state Dunham coefficients. A minimum of the functional (7) was searched by the modified Levenberg-Marquardt algorithm combined with a finite-difference approximation to the corresponding

TABLE I. MPPT potential curves of the NaRb molecule (in cm^{-1}). The energy zero is the T_e value of the *ab initio* ground-state potential.

R (a.u.)	$X\,^1\Sigma^+$	$A\,^1\Sigma^+$	$B\,^1\Pi$	$C\,^1\Sigma^+$	$D\,^1\Pi$	$E\,^1\Sigma^+$
5.4	2664	17926	20772	23482	24117	26698
5.9	998	15426	18724	21130	22149	24380
6.4	192	13716	17451	19506	20807	22937
6.9	2	12655	16769	18477	19997	22162
7.4	237	12015	16457	17839	19545	21829
7.9	734	11763	16429	17557	19429	21823
8.4	1340	11708	16506	17456	19483	21719
8.9	1980	11812	16660	17512	19691	21520
9.4	2603	12025	16831	17678	19998	21397
9.9	3186	12322	16974	17939	20321	21336
10.4	3673	12660	17107	18237	20629	21268
10.9	4082	13043	17228	18586	20920	21221
11.5	4469	13543	17362	19037	21209	21156
12.1	4751	14066	17463	19479	21421	21093
12.65	4942	14557	17542	19867	21561	21043
13.25	5091	15078	17612	20235	21651	21011

R (a.u.)	$a\,^3\Sigma^+$	$b\,^3\Pi$	$c\,^3\Sigma^+$	$d\,^3\Pi$	$e\,^3\Sigma^+$
5.4	11531	13415	22890	24032	24769
5.9	9306	11923	19979	21991	22530
6.4	7759	11210	17934	20631	21144
6.9	6739	11060	16655	19836	20394
7.4	6030	11302	15867	19396	20058
7.9	5629	11804	15518	19260	20074
8.4	5353	12436	15386	19261	20273
8.9	5204	13147	15427	19378	20603
9.4	5128	13870	15571	19573	20984
9.9	5115	14574	15777	19765	21331
10.4	5110	15217	15994	19984	21643
10.9	5130	15789	16212	20225	21826
11.5	5169	16364	16463	20535	21907
12.1	5207	16798	16690	20837	21905
12.65	5245	17099	16875	21091	21875
13.25	5282	17330	17050	21319	21849

Jacobian matrix. The $A_{ij}^{v'J'v''J''}$ coefficients were evaluated basing on the present *ab initio* MPPT transition dipole moment function $\mu_{D\,^1\Pi-X\,^1\Sigma^+}(R)$, while the rovibronic term values $T_{D\,^1\Pi}^{cal}$, as well as the wave functions $|v_J\rangle$ for the ground $X\,^1\Sigma^+$ and excited $D\,^1\Pi$ state have been obtained by a numerical solution of the radial Schrödinger equation with the RKR potentials constructed by means of the isotope-substituted Dunham molecular constants. The ground-state molecular constants were taken from Ref. [5].

III. RESULTS AND DISCUSSION

A. Electronic structure parameters

Energy curves. The potential-energy curves, see Fig. 1 and Table I, were calculated by the MPPT method for all

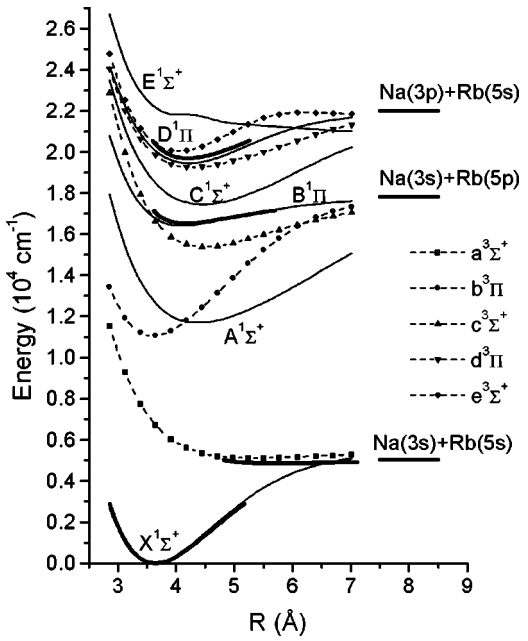

FIG. 1. The MPPT potential-energy curves for the low-lying singlet (solid lines) and triplet (dashed lines) states of NaRb. The empirical RKR potentials for the $X\,^1\Sigma^+$ [5], $a\,^3\Sigma^+$ [5], $B\,^1\Pi$ [2], and $D\,^1\Pi$ (present) states are depicted by bold solid lines.

singlet and triplet states of NaRb converging to the first three nonrelativistic dissociation limits, as well as for the $E\,^1\Sigma^+$ state converging to the $\mathrm{Na}(3s)+\mathrm{Rb}(4d)$ dissociation limit. The computed bonding energies are expected to be slightly overestimated because of basis-set superposition errors, as is mostly pronounced for the $a\,^3\Sigma$ state, see Fig. 1. One should note that these errors arise essentially from the basis-set dependencies of huge intracore correlation energies and thus should not effect the potential difference ΔU values employed in present calculations. The reliability of the derived curves can be tested by their comparison with the available experimental [2,5] and preceding *ab initio* [7,25] data. Figure 1 and Table II demonstrate that the present potentials are in satisfactory agreement with the empirical RKR curves and the corresponding experimental molecular constants for the $X\,^1\Sigma^+$, $a\,^3\Sigma^+$, $B\,^1\Pi$, and $D\,^1\Pi$ states, as well as with the recent calculations [7]. In a number of cases the present calculations are in somewhat better agreement with experimental data. For instance, for the $B\,^1\Pi$ state the relative difference $\delta(\omega_e)$ between the calculated and measured [2] vibrational constants is ca. 4% in the present work and ca. 16% in Ref. [7].

Transition moment functions. The resulting MPPT transition moments obtained in a dipole-length approximation for the most essential singlet-singlet electronic transitions are presented in Table III. The dipole moment functions for the $B\,^1\Pi\rightarrow X\,^1\Sigma^+$ and $D\,^1\Pi\rightarrow X\,^1\Sigma^+$ transitions are depicted in Fig. 2 (full symbols), along with the MPPT $\mu_{\Pi\Sigma^+}(R)$ functions extracted from the difference of the MPPT L-uncoupling matrix elements for different isotopomers according to Eq. (1) (open symbols). As can be seen, except for the small R region, the latter are in good agreement with their *ab initio* counterparts calculated directly in dipole-

TABLE II. Comparision of the experimental and *ab initio* molecular constants for the $X\,^1\Sigma^+$, $a\,^3\Sigma^+$, $B\,^1\Pi$, and $D\,^1\Pi$ states of $^{23}Na^{85}Rb$. (Energies are in cm^{-1}, R_e in Å .)

		Experimental	*Ab initio*		
		Ref. [2,5]	Present	Ref. [7]	Ref. [25]
$X\,^1\Sigma^+$	R_e	3.6435	3.62	3.71	3.63
	ω_e	106.86	107.3	103.9	106.0
$a\,^3\Sigma^+$	T_e	4847.75	5110	4363	
	R_e	5.75	5.46	5.94	
	ω_e	18.8	21.7	15.3	
$B\,^1\Pi$	T_e	16527.79	16420	16321	
	R_e	4.1767	4.08	4.34	
	ω_e	61.17	58.8	51.6	

		Experimental		*Ab initio*	
		Ref. [6]	Present	Present	Ref. [7]
$D\,^1\Pi$	T_e	19695	19692.06	19475	19529
	R_e	4.139	4.2155	4.22	4.31
	ω_e	73.5	73.26	70.3	71.9
	$\omega_e x_e$	0.459	0.4744		
	$\omega_e y_e$		0.8297×10^{-2}		
	B_e	0.0544	0.05244		
	α_e	0.36×10^{-3}	0.3311×10^{-3}		
	γ_e		0.9350×10^{-6}		

length approximation. The divergence of these two approaches in the small R region seems to be attributed to the small values of the $\xi=\xi(R)$ functions in Eq. (1) that become comparable with the absolute accuracy of the difference in the isotope-substituted L-uncoupling matrix elements at $R<4$ Å. As can be seen from Fig. 2, the $B\,^1\Pi\rightarrow X\,^1\Sigma^+$ transition dipole moment function $\mu_{B\,^1\Pi-X\,^1\Sigma^+}$ does not exhibit

TABLE III. MPPT transition dipole moment functions.

R (a.u.)	$\mu(R)$ (a.u.)					
	A-X	*B-X*	*C-X*	*D-X*	*D-A*	*D-B*
5.4	3.589	3.176	0.918	0.792	1.588	1.977
5.9	3.694	3.141	0.914	0.950	1.698	2.248
6.4	3.814	3.111	0.941	1.094	1.735	2.402
6.9	3.939	3.078	0.997	1.252	1.694	2.403
7.4	4.076	3.035	1.083	1.447	1.584	2.252
7.9	4.197	2.974	1.191	1.662	1.434	1.968
8.4	4.304	2.897	1.321	1.892	1.258	1.581
8.9	4.377	2.812	1.461	2.107	1.079	1.175
9.4	4.408	2.739	1.605	2.288	0.913	0.803
9.9	4.394	2.663	1.739	2.458	0.756	0.477
10.4	4.332	2.620	1.859	2.577	0.620	0.245
10.9	4.229	2.596	1.966	2.667	0.496	0.072
11.5	4.071	2.590	2.072	2.740	0.368	-0.063
12.1	3.901	2.599	2.171	2.784	0.255	-0.151
12.65	3.753	2.612	2.268	2.810	0.165	-0.201
13.25	3.617	2.637	2.384	2.820	0.073	-0.227

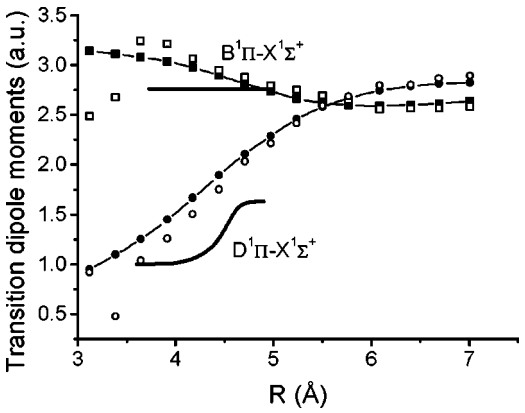

FIG. 2. The MPPT transition dipole moments $\mu_{B\,^1\Pi-X\,^1\Sigma^+}$ and $\mu_{D\,^1\Pi-X\,^1\Sigma^+}$ calculated in the dipole-length approximation (full symbols), extracted from the isotopic-substituted L-uncoupling matrix elements (open symbols). The empirical estimates from Refs. [5,6] are shown by bold solid lines.

any strong R dependence in the R interval under study. Such a behavior does not contradict the estimate $\mu(R)\approx$const at 3.73 Å$<R<$4.98 Å made in [5], the present absolute μ values being consistent with the ones obtained in Ref. [5]. For the $D\,^1\Pi\rightarrow X\,^1\Sigma^+$ transition the dipole moment function $\mu_{D\,^1\Pi-X\,^1\Sigma^+}(R)$ is steeply growing with R. A rapid increasing of μ at 4.1 Å$<R<$4.6 Å was qualitatively predicted in Ref. [6] from the failure of the Franck-Condon approximation to describe the measured intensity distribution.

L-uncoupling matrix elements. The MPPT $L_{B\,^1\Pi-N\,^1\Sigma^+}$ and $L_{D\,^1\Pi-N\,^1\Sigma^+}$ electronic matrix elements for the $^{23}Na^{85}Rb$ isotopomer, N denoting X, A, C, and E, are displayed in Fig. 3. As can be seen from Fig. 3(b), the $L_{B\,^1\Pi-A\,^1\Sigma^+}(R)$ reflects, in a wide range of R, the Van Vleck hypothesis of pure precession [26] according to which the $B\,^1\Pi-A\,^1\Sigma^+$ pair is considered as π,σ components of the $[NaRb]^+np$ complex, leading to $L_{B\,^1\Pi-A\,^1\Sigma^+}=\sqrt{2}$. The behavior of $L_{D\,^1\Pi-C\,^1\Sigma^+}$ reflects the generalized Van Vleck hypothesis of pure precession, according to which $L_{D\,^1\Pi-C\,^1\Sigma^+}$ should increase from $\sqrt{2}$ to $\sqrt{6}$ as R decreases; see Fig. 3(a). The pure precession approximation fails completely for all other matrix elements at any R range.

B. Lifetime

The radiative lifetime estimates for the $B\,^1\Pi$ and $D\,^1\Pi$ states were obtained by Eq. (5) accounting for the $B\,^1\Pi-X\,^1\Sigma^+$ transition and $D\,^1\Pi-X\,^1\Sigma^+$, $D\,^1\Pi-A\,^1\Sigma^+$, $D\,^1\Pi-B\,^1\Pi$ transitions, respectively. The contribution of the remaining $B\,^1\Pi-A\,^1\Sigma^+$ and $D\,^1\Pi-C\,^1\Sigma^+$ transitions, which were estimated by Eq. (1) from corresponding isotopic-substituted L-uncoupling matrix elements to the corresponding lifetimes is negligible because of small frequency and probability factors. The calculated v' dependences of rovibronic lifetimes τ^{Π}_{vJ} for the $B\,^1\Pi$ and $D\,^1\Pi$ states are presented in Fig. 4 for $J'=1$,50, and 100. As can be seen, the τ^{Π}_{vJ} values demonstrate pronounced sensitivity to vibrational and rotational quantum numbers, thus reflecting the strong R dependences of the $A^{sum}(R)$ operator in Eq. (5) for both states.

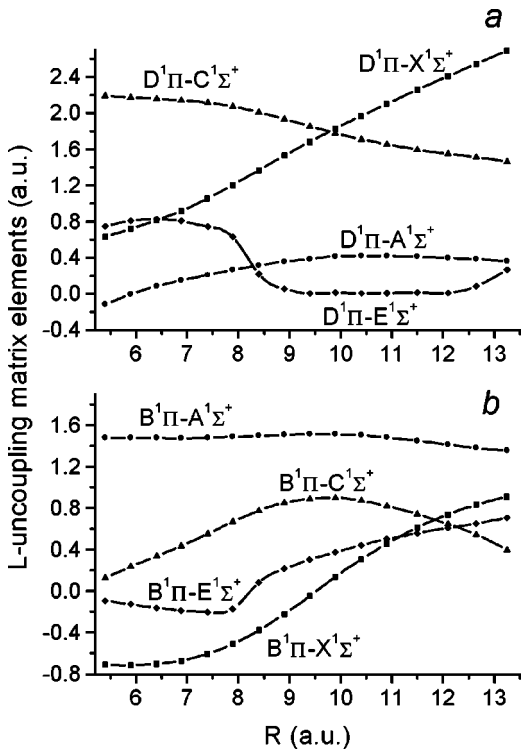

FIG. 3. The R dependence of the MPPT L-uncoupling electronic matrix elements between the $^1\Pi$ state and the first four $^1\Sigma^+$ states for the $^{23}Na^{85}Rb$ isotopomer. (a) $D\,^1\Pi$ state. (b) $B\,^1\Pi$ state.

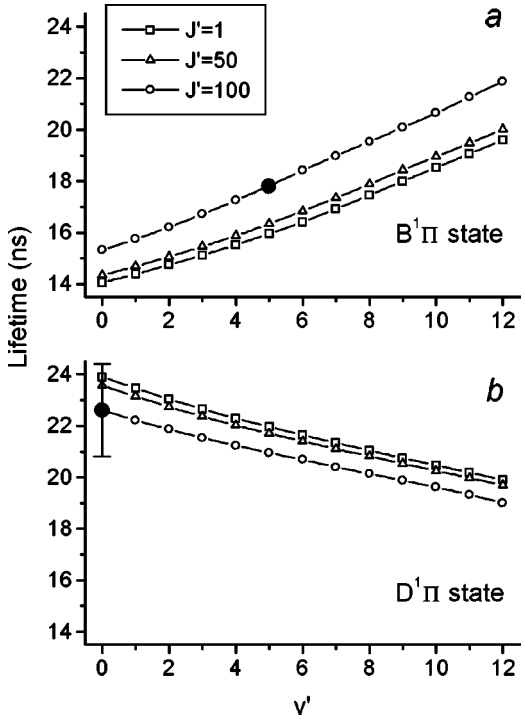

FIG. 4. The calculated radiative lifetimes of $^{23}Na^{85}Rb$ versus vibrational quantum number v' for three different rotational quantum numbers J'. (a) $B\,^1\Pi$ state. (b) $D\,^1\Pi$ state. Full circles denote the experimental lifetimes of the $B\,^1\Pi(v'=5,J'\approx 20)$ [5] and $D\,^1\Pi(v'=0,J'=44)$ [8] levels.

TABLE IV. The calculated $(q^{s\text{-}s},q^{sum})$ and experimental (q_{exp}) Λ-doubling constants (in 10^{-5} cm^{-1}) for the $B\,^1\Pi$ and $D\,^1\Pi$ states. The $q^{s\text{-}s}$ values are obtained in the singlet-singlet approximation, while q^{sum} takes into account the spin-orbit $B\,^1\Pi - c\,^3\Sigma^+$ interaction.

Isotopomer	$v'(J')$	$\lvert q_{\rm exp}\rvert$	$q^{s\text{-}s}$	q^{sum}
		$B\,^1\Pi$ state		
$^{23}Na^{85}Rb$	4(98)	0.023±0.001	-0.04	-0.02
$^{23}Na^{85}Rb$	5(116)	0.054±0.001	-0.04	-0.03
$^{23}Na^{87}Rb$	6(24)	0.29±0.03	-0.01	+0.2
$^{23}Na^{85}Rb$	8(15)	0.5 [a]	-0.01	+0.4
		$D\,^1\Pi$ state		
$^{23}Na^{85}Rb$	0(44)	0.971±0.003	+1.20	
$^{23}Na^{85}Rb$	1(7)	1.19±0.12	+1.22	
$^{23}Na^{85}Rb$	4(25)	1.08±0.03	+1.17	
$^{23}Na^{85}Rb$	4(41)	1.087±0.002	+1.16	
$^{23}Na^{87}Rb$	6(44)	1.130±0.003	+1.13	
$^{23}Na^{87}Rb$	10(36)	1.818±0.003	+1.10	
$^{23}Na^{85}Rb$	12(50)	1.091±0.001	+1.06	

[a]The q value was obtained with a ''+'' sign from the high-resolution spectroscopy data [5].

To the best of our knowledge, there exist only two spontaneous lifetime τ_{vJ} measurements in the $B\,^1\Pi$ and $D\,^1\Pi$ states of the NaRb molecule, one for a particular v,J level for each state. The value $\tau(v'=5,J'\approx 20)=17.8$ ns is reported in Ref. [5] for the $B\,^1\Pi$ state and $\tau(v'=0,J'=44)=22.6\pm 1.8$ ns is reported in Ref. [8] for the $D\,^1\Pi$ state. As can be seen from Fig. 4, the agreement between the calculated and the experimental values is quite satisfactory. It seems that the experimental τ_{vJ} value for the $B\,^1\Pi$ state slightly (for ca. 10%) exceeds its theoretical estimate, see Fig. 4(a), while the measured value for the $D\,^1\Pi$ state is somewhat 5% smaller than the theoretical one, see Fig. 4(b). Note, however, that due to the lack of experimental data it is difficult to make any definite judgment on whether the drawbacks in the calculation or the experimental inaccuracies are responsible for this discrepancy, and it is clear that a more profound experimental study is needed to test the theory.

C. Λ-doubling constants

Experimental Λ-doubling constants q_{exp} are presented in Table IV for a number of rovibronic levels of the $B\,^1\Pi$ and $D\,^1\Pi$ states. Only absolute values $|q_{exp}|$ can be deduced from the RF-ODR experiment. The errors quoted for q_{exp} are estimated from the statistical uncertainty in the resonance position of the RF-ODR signals. We added to our data for the $B\,^1\Pi$ state the q_{exp} value and sign for the level $v(J)=8(15)$, which we extracted from the high resolution spectroscopy studies reported in Ref. [5]. Note that, as follows from Ref. [5], this level is strongly locally perturbed.

Singlet-singlet approximation. The q^{Π}_{vJ} values calculated in the singlet-singlet approximation, see Eqs. (2) and (6), are given in Table IV as q^{s-s} for the $B\,^1\Pi$ and $D\,^1\Pi$ states.

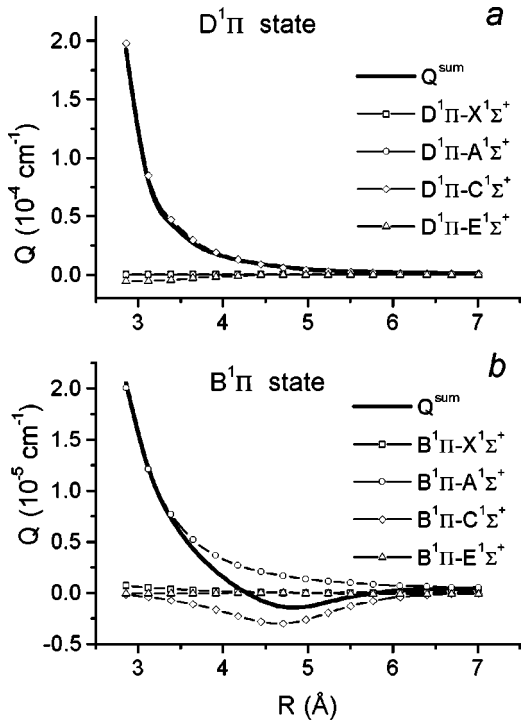

FIG. 5. The calculated according to Eq. (6) partial (Q_j) and summary (Q^{sum}, bold) contributions of the first four $^1\Sigma^+$ states into the q values of the $D\,^1\Pi$ state (a) and $B\,^1\Pi$ state (b) of $^{23}Na^{85}Rb$. The $X\,^1\Sigma^+$ and $A\,^1\Sigma^+$ contributions are almost indistinguishable.

They demonstrate pronounced sensitivity to the vibrational and rotational quantum numbers involved. This reflects the strong R dependences of the $Q^{sum}(R)$ operator in Eq. (6), see Fig. 5. The behavior of $Q^{sum}(R)$ in Fig. 5 shows that the $D\,^1\Pi$ state obeys the unique perturber approximation [27]. Moreover, the observed crossing at $R \approx 6$(Å) between the interacting $D\,^1\Pi - E\,^1\Sigma^+$ states, see Fig. 1, does not affect the q^D_{vJ} values for $v^D = 1-12$ since the L_{D-E}-uncoupling matrix element, see Fig. 3, as well as the probability densities of the corresponding vibrational wave functions are negligible near the crossing point. The q factors for the $B\,^1\Pi$ state are determined by a strong competition between the lower $A\,^1\Sigma^+$ and upper $C\,^1\Sigma^+$ state contributions leading to the extremely small q values. This fact explains why Λ splitting in the $B\,^1\Pi$ state was not observed for the unperturbed levels in the high-resolution spectroscopy studies [2].

The q factors in the $D\,^1\Pi$ state, being about 1×10^{-5} cm^{-1}, are much larger than the ones in the $B\,^1\Pi$ state. As follows from Table IV, the calculated $D\,^1\Pi$ state q factors q^{s-s} are in good agreement with the experimental ones in a wide range of $v'(J')$ levels, except for the level $v'(J') = 10(36)$, in which q_{exp} exceeds the calculated value by a factor of almost two. The comparison of q^{s-s} and q_{exp} values for the $B\,^1\Pi$ state shows less consistency, which can be probably attributed to the effect of local perturbations.

Singlet-triplet perturbation effect. The spin-orbit (SO) interaction $B\,^1\Pi - c\,^3\Sigma^+$ mixes the $B\,^1\Pi$ ($S=0, \Omega=\Lambda=\pm1$) state with the $^3\Sigma_1^+$ ($S=1, \Omega=\Sigma=\pm1$) components of the crossing $c\,^3\Sigma^+$ state, see Fig. 1. In the framework of the simplest two-level model, the e-parity levels of the perturbed $B\,^1\Pi$ state interact with the $^3\Sigma_0^+$ ($S=1, \Omega=\Sigma=0$) component of the $c\,^3\Sigma^+$ state due to the S-uncoupling matrix element $C^{s-t}\sqrt{J(J+1)}/MR^2$, where C^{s-t} is the mixing coefficient corresponding to a fraction of the $c\,^3\Sigma^+$ state in the perturbed $B\,^1\Pi$ state wave function [23]. Then, assuming the regularity of the spin-rotational perturbation, the contribution q^{s-t} of the singlet-triplet $B\,^1\Pi - c\,^3\Sigma^+$ interaction into the q factors of the $B\,^1\Pi$ state is roughly reduced by the sum rule (6) to the form

$$q^{s-t} = \frac{1}{M^2}\langle v_J^{\Pi}| \frac{1}{\lambda R^4}\left(\frac{1-\Delta U_{B-c}/\lambda}{1+\Delta U_{B-c}/\lambda}\right)|v_J^{\Pi}\rangle, \qquad (8)$$

where $\lambda(R) = \sqrt{\Delta U^2_{B-c} + 4V^2_{so}}$ and $V_{so}(R)$ is the $B\,^1\Pi \sim c\,^3\Sigma^+$ SO matrix element. The required $V_{so}^{NaRb}(R)$ function was estimated from the corresponding *ab initio* $V_{so}^{NaK}(R)$ function for the NaK molecule [28] which was scaled by the ratio of the experimental SO constants of Rb and K atoms [29]: $V_{so}^{NaRb}(R) = V_{so}^{NaK}(R)\varsigma_{so}^{Rb}/\varsigma_{so}^{K}$, where $\varsigma_{so}^{Rb} = 158$ cm^{-1}, $\varsigma_{so}^{K} = 38$ cm^{-1}. In spite of the crude model used, the resulting q factors $q^{sum} = q^{s-s} + q^{s-t}$ presented in Table IV are in reasonable agreement with their experimental analogs, especially taking into account the small values of the $B\,^1\Pi$ state q factors. The possible SO $B\,^1\Pi - b\,^3\Pi$ perturbation effect on the q factors of the $B\,^1\Pi$ state is expected to be much less pronounced than the $B\,^1\Pi - c\,^3\Sigma^+$ one since its influence appears only in the third order of the nondegenerate perturbation theory. Moreover, Fig. 1 induces one to assume that the overlap integrals between vibrational wave functions of the $B\,^1\Pi$ and $b\,^3\Pi$ states are negligible for the low v_B levels, thus assignment of a number of local $B\,^1\Pi$ state perturbations to a direct $B\,^1\Pi - b\,^3\Pi$ SO interaction [3] seems to be questionable. It should also be added that in Hund's case (c) coupling representation the difference in perturbation effects caused by the $^3\Pi_1$ and $^3\Sigma_1$ components becomes indistinguishable.

Although an admixture of the triplet $d\,^3\Pi$ and $e\,^3\Sigma^+$ electronic wave functions to the $D\,^1\Pi$ state wave function seems to be of lesser importance than for the $B\,^1\Pi$ state because of much smaller SO effects in the Na($3p$) atom as compared to Rb($5p$), the local singlet-triplet interaction could be responsible for the relatively small irregular changes of the measured q^{Π}_{vJ} factor, see Table IV.

D. Refinement of the $D\,^1\Pi$ potential

The relative intensity distributions in the $D\,^1\Pi \rightarrow X\,^1\Sigma^+$ LIF progressions resulting from the fixed $D\,^1\Pi$ state vibrational-rotational levels $v'(J')$ measured in the present work, namely 0(44), 1(104), 4(25), 6(44), 6(120), 10(36) and 12(50) are presented in Fig. 6 (open bars), along with the $v'(J')$ equal to 0(44), 5(62), 6(44) from Ref. [6] (striped bars). Table V contains the experimentally determined term values $T^{exp}_{v'J'}$, obtained by adding the wave numbers of Ar^+ laser lines causing $D\,^1\Pi(v',J') \leftarrow X\,^1\Sigma^+(v'',J'')$ transitions

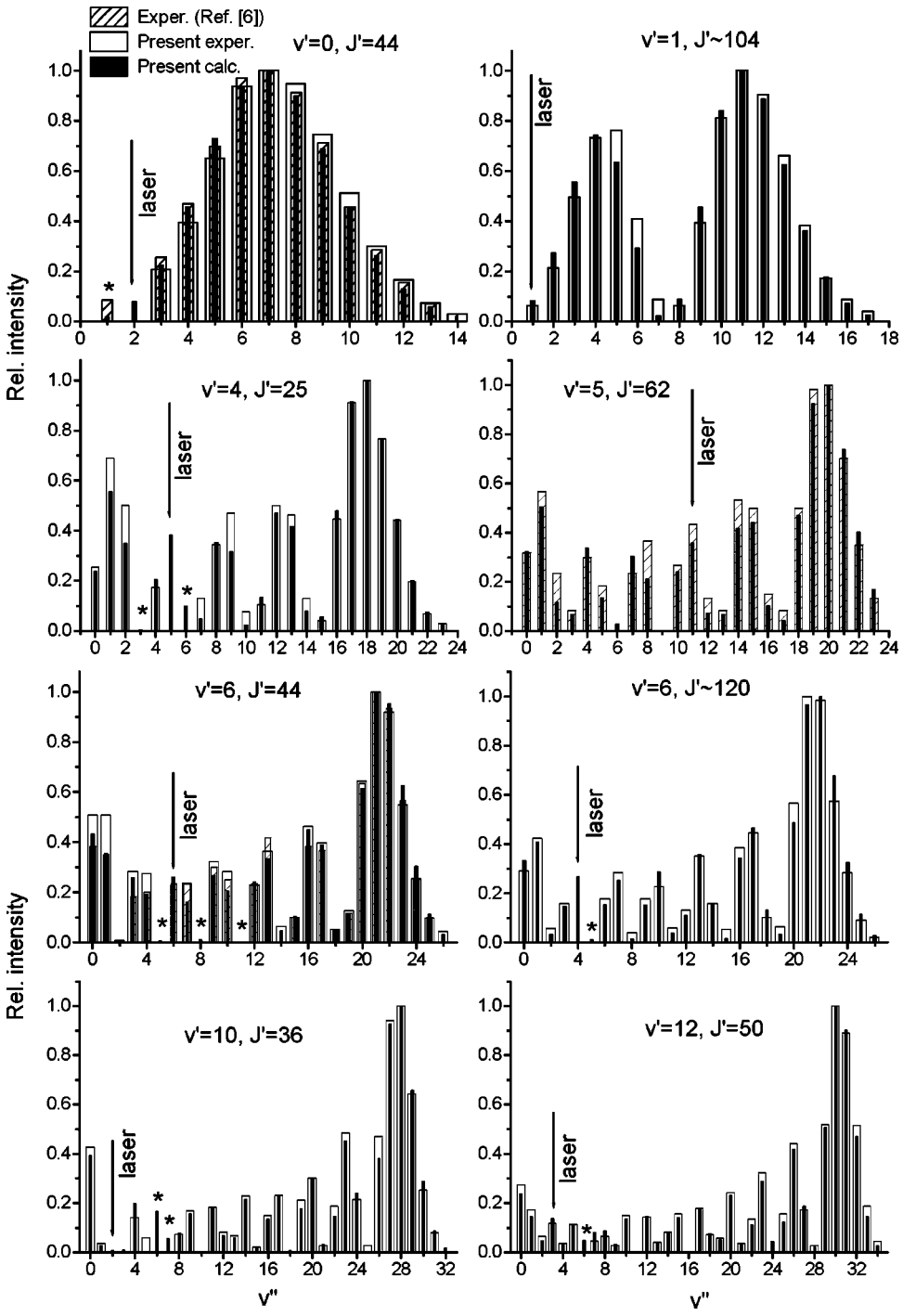

FIG. 6. Comparison of the preceding [6] and present measured relative intensity distributions in the $D\,^1\Pi(v',J')\rightarrow X\,^1\Sigma^+$ LIF progressions with their theoretical analogs. Both measured and calculated probabilities for each progression were normalized to 1 for the band having maximum intensity. (*) — intensity could not be determined due to overlapping with other lines.

to the corresponding $X^1\Sigma^+(v'',J'')$ energies, which were calculated by means of Dunham constants from Ref. [5]. Term values with $J'\geqslant 100$ are not presented in Table V since their accuracy is insufficient due to still unknown centrifugal-distortion constants of the $X\,^1\Sigma^+$ state, hence, the J' assignment is not unambigious for large J' values.

The measured intensity distributions and term values were involved in the simultaneous nonlinear fitting procedure, see Eq. (7), to produce the refined molecular constant set for the $D\,^1\Pi$ state of the $^{23}Na^{85}Rb$ molecule. Three different initial sets of the $D\,^1\Pi$ state molecular constants were used, namely, the constants given in Ref. [6], as well as the constants estimated from the present and preceding [7] *ab initio* potentials. The independence of the final set of the molecular constants of the choice of the initial sets guarantees the achievement of the global minimum of the functional (7). The refined $D\,^1\Pi$ state molecular constants are given in Table II, while the corresponding RKR potential is depicted in Fig. 1 (solid bold line). The calculated relative intensity distributions are displayed in Fig. 6 (full bars). As follows from Fig. 6, the present experimental and theoretical intensities are in satisfactory agreement, especially for high vibrational levels v'. They agree with the preceding intensity distributions measured by Takahashi and Katô [6], which are

TABLE V. Experimental $D\,^1\Pi$ state term values $T_{v'J'}$. λ_{exc} is the exciting laser wavelength (in nm) and Δ_{o-c} is the difference between the observed term values and the term values calculated using either the present constant set ($\Delta_{o-c}^{present}$) or the constants given in Ref. [6] ($\Delta_{o-c}^{\text{Ref. [6]}}$). $T_{v'J'}$ and Δ_{o-c} are in cm^{-1}.

Isotopomer	$v',J' \leftarrow v'',J''$	λ_{exc}	$T_{v'J'}^{exp}$	$\Delta_{o-c}^{present}$	$\Delta_{o-c}^{\text{Ref. [6]}}$
$^{23}Na^{85}Rb$	0,44←2,44	514.5	19831.53	0.07	9.53
$^{23}Na^{85}Rb$	1,7←3,8	514.5	19804.03	-0.24	13.80
$^{23}Na^{85}Rb$	4,25←5,24	514.5	20042.02	-0.94	13.13
$^{23}Na^{85}Rb$	4,41←0,41	501.7	20099.61	0.68	9.27
$^{23}Na^{87}Rb$	6,44←6,45	514.5	20248.61	1.72	8.53
$^{23}Na^{87}Rb$	10,36←2,35	496.5	20472.87	-4.24	21.40
$^{23}Na^{85}Rb$	12,50←3,49	496.5	20673.00	-0.19	20.21

also depicted in Fig. 6 (striped bars) when available. The $D\,^1\Pi$ state rovibronic term values $T_{v'J'}$ calculated with the refined molecular constants from the Table II reproduce their experimental counterparts much better than the calculations based on the previous constants from Ref. [6], cf. the differences Δ_{o-c} between the observed and calculated $T_{v'J'}$ values in Table V. The maximum deviation between the theoretical and experimental term values has been obtained for the level $v'=10, J'=36$, which seems to be locally perturbed by the near-lying $d\,^3\Pi$ and/or $e\,^3\Sigma^+$ state, see Fig. 1. Note that it is just this level possessing the largest deviation between the observed and calculated q factor, see Table IV.

It is worth mentioning that the refinement of the $D\,^1\Pi$ state molecular constants is achieved mainly through the improvement of the rotational constants. Indeed, the changes in B_e are ca. 4%, while ω_e was changed only by ca. 0.3%, see Table II. This can be clearly understood from the fact that the Franck-Condon factors are more sensitive to the variation of the rotational constants than to the vibrational ones.

IV. CONCLUDING REMARKS

The MPPT calculation method previously used to estimate the NaRb permanent electric dipoles [9] has been successfully applied to evaluate the energy and radiative properties of the NaRb molecule. Further improvement of the theoretical treatment apparently demands an explicit consideration of overall singlet-triplet interactions based on relativistic calculations of the spin-orbit matrix elements [28]. The *ab initio* calculations required are currently in progress.

The paper demonstrates that in the case when only few experimental term values of the upper state are available, an improvement of the molecular constant set can be achieved by including the relative LIF intensities into the simultaneous fitting routine. The required accurate transition dipole moment functions can be obtained as the *ab initio* MPPT estimates.

The calculated transition moments $\mu(R)$ and L-uncoupling matrix elements of NaRb are very close to the corresponding $\mu(R)$ and $L(R)$ functions of the NaK molecule [14,15]. The minor changes of $\tau_{v'J'}$ and $q_{v'J'}$ in passing from NaK to NaRb can be attributed to the mass dependence, small relative position changes of the interacting electronic states, as well as to the more pronounced SO effects.

ACKNOWLEDGMENTS

Financial support by the Russian Fund of Fundamental Research under Grants No. 00-03-32978 and No. 00-03-33004 is gratefully acknowledged by the Moscow group. The Riga group appreciates the financial support from the Latvian Science Council under Grant No. 96.0323. O.N. is grateful for the support from the Latvian Science Council Doctoral Studies Grant No. 44. R.C. gratefully acknowledges support from the Italian MURST (Grant No. 9803246-003). The authors are grateful to Professor W. C. Stwalley for useful discussions.

[1] H. Wang and W. C. Stwalley, J. Chem. Phys. **108**, 5767 (1998).
[2] Y.-C. Wang, M. Kajitani, S. Kasahara, M. Baba, K. Ishikawa, and H. Katô, J. Chem. Phys. **95**, 6229 (1991).
[3] Y.-C. Wang, K. Matsubara, and H. Katô, J. Chem. Phys. **97**, 811 (1992).
[4] K. Matsubara, Y.-C. Wang, K. Ishikawa, M. Baba, A. J. McCaffery, and H. Katô, J. Chem. Phys. **99**, 5036 (1993).
[5] S. Kasahara, T. Ebi, M. Tanimura, H. Ikoma, K. Matsubara, M. Baba, and H. Katô, J. Chem. Phys. **105**, 1341 (1996).
[6] N. Takahashi and H. Katô, J. Chem. Phys. **75**, 4350 (1981).
[7] M. Korek, A. R. Allouche, M. Kobeissi, A. Chaalan, M. Dagher, K. Fakherddin, and M. Aubert-Frecon, Chem. Phys. **256**, 1 (2000).
[8] M. Jansons, J. Klavins, Z. Kharcheva, and M. Tamanis, Phys. Scr. **45**, 328 (1992).
[9] O. Nikolayeva, I. Klincare, M. Auzinsh, M. Tamanis, R. Ferber, E. A. Pazyuk, A. V. Stolyarov, A. Zaitsevski, and R. Cimiraglia, J. Chem. Phys. **113**, 4896 (2000).
[10] J. M. Walter and S. Barrat, Proc. R. Soc. London, Ser. A **119**, 257 (1928).
[11] A. Zaitsevskii and J. P. Malrieu, Theor. Chem. Acc. **96**, 269 (1997).
[12] A. Zaitsevskii and R. Cimiraglia, Int. J. Quantum Chem. **73**, 395 (1999).
[13] M. Tamanis, M. Auzinsh, I. Klincare, O. Nikolayeva, R. Ferber, E. A. Pazyuk, A. V. Stolyarov, and A. Zaitsevskii, Phys. Rev. A **58**, 1932 (1998).
[14] M. Tamanis, M. Auzinsh, I. Klincare, O. Nikolayeva, R. Ferber, A. Zaitsevskii, E. A. Pazyuk, and A. V. Stolyarov, J. Chem. Phys. **109**, 6725 (1998).
[15] S. O. Adamson, A. Zaitsevskii, E. A. Pazyuk, A. V. Stolyarov, M. Tamanis, R. Ferber, and R. Cimiraglia, J. Chem. Phys. **113**, 8589 (2000).
[16] A. V. Stolyarov and V. I. Pupyshev, Phys. Rev. A **49**, 1693 (1994).

[17] S. J. Silvers, T. H. Bergeman, and W. Klemperer, J. Chem. Phys. **52**, 4385 (1970).
[18] R. W. Field and T. H. Bergeman, J. Chem. Phys. **54**, 2936 (1971).
[19] G. Audi and A. M. Wapstra, Nucl. Phys. A **595**, 409 (1995).
[20] M. Mizushima, *Theory of Rotating Diatomic Molecules* (Wiley and Sons, New York, 1975).
[21] L. F. Pacios and P. A. Christiansen, J. Chem. Phys. **82**, 2664 (1985).
[22] L. A. LaJohn, P. A. Christiansen, R. B. Ross, T. Atashroo, and W. C. Ermler, J. Chem. Phys. **87**, 2812 (1987).
[23] H. Lefebvre-Brion and R. W. Field, *Perturbations in the Spectra of Diatomic Molecules* (Academic, New York, 1986).
[24] E. A. Pazyuk, A. V. Stolyarov, and V. I. Pupyshev, Chem. Phys. Lett. **228**, 219 (1994).
[25] G. Igel-Mann, U. Weding, P. Fuentealta, and H. Stoll, J. Chem. Phys. **84**, 5007 (1986).
[26] J. H. van Vleck, Phys. Rev. **33**, 467 (1929).
[27] R. N. Zare, A. L. Schmeltekopf, W. J. Harrop, and D. L. Albritton, J. Mol. Spectrosc. **46**, 37 (1973).
[28] R. Ferber, E. A. Pazyuk, A. V. Stolyarov, A. Zaitsevskii, P. Kowalczyk, Hongmin Chen, He Wang, and W. C. Stwalley, J. Chem. Phys. **112**, 5740 (2000).
[29] W. L. Wiese, M. W. Smith, and B. M. Miles, *Atomic Transition Probabilities* Natl. Stand. Ref. Data Ser. Natl. Bur. Stand. (U.S.) Circ. No. 22 (U.S. GPO, Washington, DC, 1969), Vol. 2.